

# Evaluation of Tin–Oxygen Bond Association by Means of *ab Initio* Molecular Orbital Calculations

Kan Wakamatsu,<sup>\*,†</sup> Akihiro Orita,<sup>‡</sup> and Junzo Otera<sup>\*,‡</sup>

Department of Chemistry and Department of Applied Chemistry, Okayama University of Science, Ridai-cho, Okayama 700-005, Japan

Received November 25, 2007

*Ab initio* calculations with MP2 provide reliable information about structure and bonding of organotin molecules. The association behavior of organotin alkoxides is counterbalanced by conflicting enthalpy and entropy contributions. The increase in Lewis acidity of tin induced by attachment of alkoxy group(s) is of prime importance for the association. On the other hand, formation of the stable dimeric distannoxanes has been proved by great negative  $\Delta G$  values. The oxygen atom between the tin atoms in distannoxanes has stronger Lewis basicity than that in organotin alkoxides. The multiplier effect of both Lewis acidity of tin and Lewis basicity of oxygen is reflected on the shortening of the secondary Sn–O bond. As a whole, tin–oxygen bonds have been successfully elucidated for the first time by *ab initio* calculations.

## Introduction

The association of tin–oxygen bonds to form tin–oxygen cycles plays a crucial role for determining structural features of organotin compounds.<sup>1</sup> It is well-known that organotin alkoxides undergo aggregation leading to dimers, or higher oligomers on occasion.<sup>2</sup> Moreover, 1,3-disubstituted tetraalkyl-distannoxanes experience dimerization to form a unique ladder structure through a tin–oxygen coordination bond.<sup>3</sup> Such characteristic association is reflected on not only structural profiles but also unique reactivities. For instance, the tin–alkoxy bond undergoes facile insertion reaction with heterocumulenes.<sup>1</sup> In particular, reaction with carbon dioxide is currently receiving extensive attention as a phosgene-free protocol for synthesizing alkyl carbonates, which are key starting materials for commercial production of isocyanates and polycarbonates.<sup>4</sup> On the other hand, the distannoxanes exhibit high catalytic activities for carbonyl activation like transesterification owing to the template effects induced by the dimerization.<sup>5</sup> The association behavior

Scheme 1



of organotin alkoxides in solution was well studied,<sup>6</sup> and the dimeric ladder formulation was confirmed for a considerable number of distannoxanes on the basis of X-ray analysis,<sup>7</sup> molecular weight measurements,<sup>8</sup> and <sup>119</sup>Sn NMR spectroscopy.<sup>9,10</sup> Despite such extensive studies, the tin–oxygen coordination bond itself has not been fully elucidated. Herein, we invoke *ab initio* molecular orbital calculations to get deeper insight into the association of tin–oxygen bonds in the organotin alkoxides and distannoxanes.

\* Address correspondence to these authors.

† Department of Chemistry.

‡ Department of Applied Chemistry.

(1) (a) Davies, A. G. *Organotin Chemistry*, 2nd ed.; Wiley-VCH: Weinheim, Germany, 2004; Chapters 12 and 14. (b) Pereyre, M.; Quintard, J.-P.; Rahm, A. *Tin in Organic Synthesis*; Butterworths: London, UK, 1987; Chapter 11.

(2) (a) Bloodworth, A. J.; Davies, A. G. In *Organotin Compounds*; Sawyer, A. K., Ed.; Marcel Dekker, INC.: New York, 1971; Vol. 1, p 153. (b) Chandrasekhar, V.; Nagendran, S.; Baskar, V. *Coord. Chem. Rev.* **2002**, 235, 1.

(3) (a) Okawara, R.; Wada, M. *Adv. Organomet. Chem.* **1967**, 5, 137. (b) Okawara, R.; Otera, M. In *Organotin Compounds*; Sawyer, A. K., Ed.; Marcel Dekker, INC.: New York, 1972; Vol. 2, p 253.

(4) (a) Kizlink, J.; Pastucha, I. *Collect. Czech., Chem. Commun.* **1994**, 59, 2116. (b) Choi, J.-C.; Sakakura, T.; Sako, T. *J. Am. Chem. Soc.* **1999**, 121, 3793. (c) Sakakura, T.; Choi, J.-C.; Saito, Y.; Masuda, T.; Sako, T.; Oriyama, T. *J. Org. Chem.* **1999**, 64, 4506. (d) Ballivet-Tkatchenko, D.; Douteau, O.; Stutzmann, S. *Organometallics* **2000**, 19, 4563. (e) Ballivet-Tkatchenko, D.; Jerphagnon, T.; Ligabue, R.; Plasseraud, L.; Poinsot, D. *Appl. Catal. A* **2003**, 255, 93. (f) Zheng, G.-L.; Ma, J.-F.; Yang, J.; Li, Y.-Y.; Hao, X.-R. *Chem. Eur. J.* **2004**, 10, 3761. (g) Ballivet-Tkatchenko, D.; Burgat, R.; Chambrey, S.; Plasseraud, L.; Richard, P. *J. Organomet. Chem.* **2006**, 691, 1498.

(5) (a) Otera, J. *Chem. Rev.* **1993**, 93, 1449. (b) Otera, J. In *Advances in Detailed Reaction Mechanisms*; Coxon, J. M., Ed.; JAI: London, UK, 1994; p 167. (c) Otera, J. *Acc. Chem. Res.* **2004**, 37, 288.

(6) (a) Smith, P. J.; White, R. F. M. *J. Organomet. Chem.* **1972**, 40, 341. (b) Davies, A. G.; Kleinschmidt, D. C.; Palan, P. R.; Vasishtha, S. C. *J. Chem. Soc. (C)* **1971**, 3972. (c) Kennedy, J. D.; McFarlane, W.; Smith, P. J.; White, R. F. M. *J. Chem. Soc., Perkin II* **1973**, 1785.

(7) (a) Chow, Y. M. *Inorg. Chem.* **1971**, 10, 673. (b) Garner, C. D.; Hughs, B. *Inorg. Nucl. Chem. Lett.* **1976**, 12, 859. (c) Graziani, R.; Bombieri, G.; Forsellini, E. *J. Organomet. Chem.* **1977**, 125, 43. (d) Harrison, P. G.; Begley, M. J.; Molloy, K. C. *J. Organomet. Chem.* **1980**, 186, 213. (e) Puff, H.; Friedrichs, E.; Visel, F. *Z. Anorg. Allg. Chem.* **1981**, 477, 50. (f) Puff, H.; Bung, I.; Friedrichs, E.; Jansen, A. *J. Organomet. Chem.* **1983**, 254, 23. (g) Vollano, J. F.; Day, R. O.; Holmes, R. R. *Organometallics* **1984**, 3, 745. (h) Schoop, T.; Roesky, H. W.; Noltemeyer, M.; Schmidt, H.-G. *Organometallics* **1993**, 12, 571. (i) Ribot, F.; Sanchez, C.; Meddour, A.; Gielen, M.; Tiekink, E. R. T.; Biesemans, M.; Willem, R. *J. Organomet. Chem.* **1998**, 552, 177. (j) Primel, O.; Llauro, M.-F.; Pétiard, R.; Michel, A. *J. Organomet. Chem.* **1998**, 558, 19. (k) Beckmann, J.; Jurkschat, K.; Rabe, S.; Schürmann, M.; Dakternieks, D. *Z. Anorg. Allg. Chem.* **2001**, 627, 458. (l) Beckmann, J.; Dakternieks, D.; Duthie, A.; Mitchell, C. *Appl. Organomet. Chem.* **2004**, 18, 51.

(8) (a) Wada, M.; Nishino, M.; Okawara, R. *J. Organomet. Chem.* **1965**, 3, 70. (b) Maeda, Y.; Okawara, R. *J. Organomet. Chem.* **1967**, 10, 247.

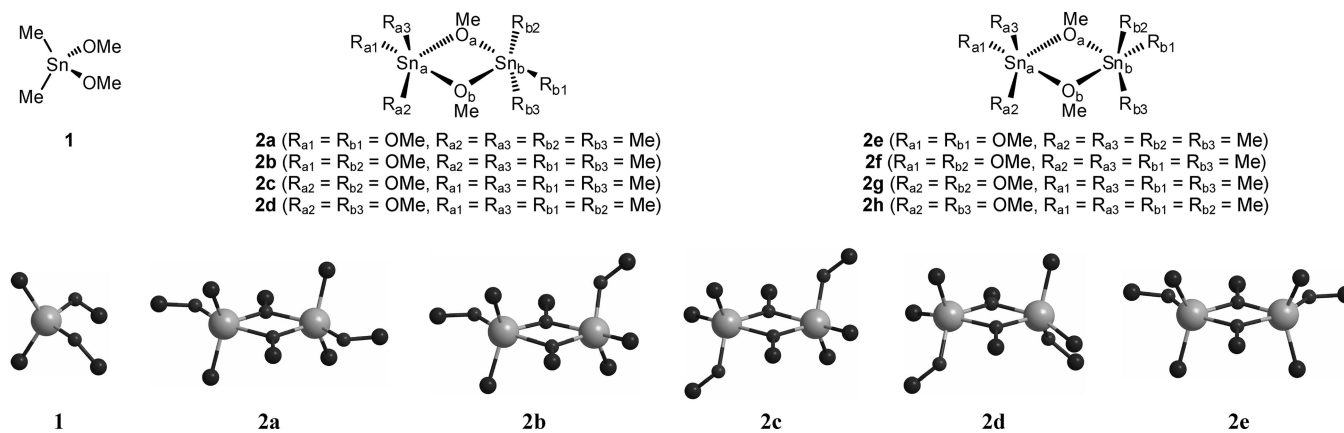
(9) (a) Otera, J.; Yano, T.; Nakashima, K.; Okawara, R. *Chem. Lett.* **1984**, 2109. (b) Yano, T.; Nakashima, K.; Otera, J.; Okawara, R. *Organometallics* **1985**, 4, 1501.

(10) (a) Two monomeric species are known for distannoxanes with extremely bulky alkyl groups: Edelman, M. A.; Hitchcock, P. B.; Lappert, M. F. *J. Chem. Soc., Chem. Commun.* **1990**, 1116. (b) Kašná, B.; Jambor, R.; Schürmann, M.; Jurkschat, K. *J. Organomet. Chem.* **2007**, 692, 3555.

**Table 1. Atomic Distances in Dimethyltin Dimethoxide Dimer (2a) and Thermochemical Parameters In the Dimerization of the Monomer 1 to 2a**

calculation level of theory	atomic distance/Å				BSSE/ kcal mol <sup>-1</sup>	TΔS/ kcal mol <sup>-1</sup>	ΔH <sub>corr</sub> <sup>a</sup> / kcal mol <sup>-1</sup>	ΔG <sub>corr</sub> <sup>a</sup> / kcal mol <sup>-1</sup>
	Sn <sub>a</sub> –O <sub>a</sub>	Sn <sub>a</sub> –O <sub>b</sub>	Sn <sub>a</sub> –O <sub>a'</sub>	Sn–C				
experimental <sup>b</sup>	2.0385	2.3246	2.0387	2.1308, 2.1219				
B3LYP/6-31G*-LANL2DZ(Sn)	2.0252	2.2591	1.9819	2.1356, 2.1347	8.48	-17.10	-10.89	6.21
B3LYP/6-31+G*-LANL2DZ(Sn)	2.0271	2.2792	1.9936	2.1385, 2.1367	2.40	-16.24	-13.21	3.03
B3LYP/6-311+G*-LANL2DZ(Sn)	2.0337	2.2618	2.0021	2.1399, 2.1398	3.47	-16.56	-16.48	0.07
B3LYP/aug-cc-pVDZ-PP	2.0759	2.3539	2.0542	2.1594, 2.1591	3.73	-14.78	-8.96	5.81
B3LYP/aug-cc-pVTZ-PP	2.0608	2.3616	2.0379	2.1529, 2.1528	0.92	-13.39	-7.87	5.52
HF/6-31G*-LANL2DZ(Sn)	1.9882	2.2637	1.9469	2.1267	6.14	-14.70	-10.47	4.22
HF/6-31+G*-LANL2DZ(Sn)	1.9882	2.2746	1.9539	2.1253	3.04	-17.18	-11.77	5.41
HF/6-311+G*-LANL2DZ(Sn)	1.9937	2.2555	1.9581	2.1216	4.27	-16.87	-14.35	2.52
MP2/6-31G*-LANL2DZ(Sn)	2.0237	2.2327	1.9802	2.1289, 2.1271	14.22	-14.78	-14.95	-0.17
MP2/6-31+G*-LANL2DZ(Sn)	2.0248	2.2436	1.9945	2.1320, 2.1310	10.77	-15.19	-18.81	-3.63
MP2/6-311+G*-LANL2DZ(Sn)	2.0274	2.2358	1.9994	2.1259, 2.1232	11.72	-13.37	-20.73	-7.37

<sup>a</sup> Corrected by BSSE. <sup>b</sup> From reference 4b.

**Figure 1.** Optimized structures of **1** and **2a–e** calculated by MP2/6-311+G\*-LANL2DZ(Sn). Hydrogen atoms are omitted for clarity.**Table 2. Dependence of Energy Change in the Dimerization on the Alkyl Chain Length<sup>a</sup>**

method	R	BSSE/kcal mol <sup>-1</sup>	ΔE <sub>corr</sub> <sup>b</sup> /kcal mol <sup>-1</sup>
B3LYP	Me	3.47	-18.14
	Et	3.59	-16.86
	Bu	3.69	-14.78
MP2	Me	11.72	-22.08
	Et	14.02	-23.88
	Bu	16.85	-24.39

<sup>a</sup> All calculations were performed with LANL2DZ for Sn and 6-311+G\* for C, H, and O atoms. <sup>b</sup> Corrected by BSSE.

### Method

The quantum chemical calculations for the organotin alkoxides and distannoxanes were carried out with the Gaussian 03 program package.<sup>11</sup> We explored a reliable calculation level of theory for energy comparison, and decided to mainly use the Møller–Plesset second-order perturbation theory (MP2) (vide infra). The hybrid density functional calculations with B3LYP functional were also applied in energy comparison among the dimers or the trimers. Because of a significant relativistic effect and unavailability of a full set of a large basis for a heavy atom, a basis set including the effective core potential (ECP) should be selected for the tin atom.

(11) Gaussian 03, Revision D.01; Frisch, M. J.; et al. Gaussian, Inc.: Wallingford, CT, 2004.

**Table 3. Single-Point Calculation Performed by Various Levels of Theory in Dimerization of 1 to 2a<sup>a</sup>**

method	BSSE/kcal mol <sup>-1</sup>	ΔE <sub>corr</sub> <sup>b</sup> /kcal mol <sup>-1</sup>
B3LYP	3.48	-17.48
B3LYP <sup>c</sup>	3.47	-18.14
HF	4.47	-16.24
HF <sup>c</sup>	4.27	-16.27
MP2	11.72	-22.08
MP3	11.84	-21.89
MP4(SDQ)	11.74	-20.77

<sup>a</sup> All calculations were performed with LANL2DZ for Sn and 6-311+G\* for C, H, and O atoms. The geometries of **1** and **2a** were optimized by MP2 except where otherwise mentioned. <sup>b</sup> Corrected by BSSE. <sup>c</sup> The geometry was optimized by the same level of theory.

In consideration for a balance between reliability and calculation efficiency, we used a combination of LANL2DZ basis set<sup>12</sup> including ECP for Sn and 6-311+G\* for other atoms. We refer to this basis set as “6-311+G\*-LANL2DZ(Sn)” in the following sections.

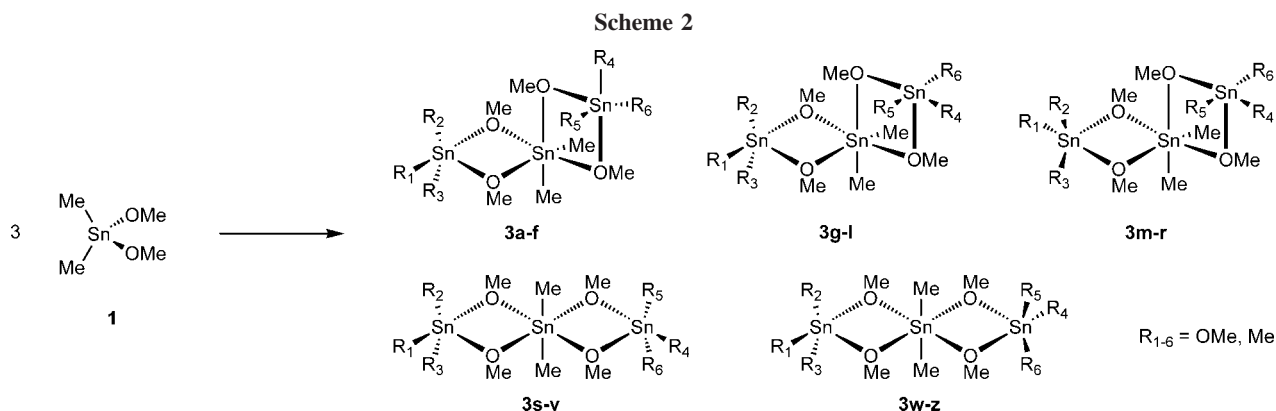
Full geometry optimizations were done with no symmetry restriction and the characterization of the stationary points was verified by the subsequent vibrational frequency analyses (no imaginary frequencies). All thermochemical parameters were evaluated at 298.15 K and 1 atm. For estimation of the energy change in dimerization of the organotin alkoxides or distannoxanes, energetic correction by a basis set superposition error (BSSE), which was evaluated by using the standard counterpoise calculation, was applied (ΔH<sub>corr</sub>, ΔG<sub>corr</sub>).<sup>13</sup> Atomic charges were determined by natural population analysis (NPA) by using MP2 density.<sup>14</sup>

(12) Hay, P. J.; Wadt, W. R. *J. Chem. Phys.* **1985**, *82*, 299.

Table 4. Calculation Results at MP2/6-311+G\*-LANL2DZ(Sn) in Dimerization of **1** to **2**<sup>a</sup>

	BSSE/kcal mol <sup>-1</sup>	<i>TΔS</i> /kcal mol <sup>-1</sup>	$\Delta H_{\text{corr}}^b$ /kcal mol <sup>-1</sup>	$\Delta G_{\text{corr}}^b$ /kcal mol <sup>-1</sup>	Sn–O/Å	
					Sn <sub>a</sub> –O <sub>a</sub> , Sn <sub>b</sub> –O <sub>b</sub>	Sn <sub>a</sub> –O <sub>b</sub> , Sn <sub>b</sub> –O <sub>a</sub>
<b>1</b>					1.9489	
<b>2a</b>	11.72	–13.37	–20.73	–7.37	2.0274	2.2358
<b>2b</b>	13.11	–16.07	–15.97	0.10	2.0208 (Sn <sub>a</sub> –O <sub>a</sub> ) 2.0551 (Sn <sub>b</sub> –O <sub>b</sub> )	2.2497 (Sn <sub>a</sub> –O <sub>b</sub> ) 2.1991 (Sn <sub>b</sub> –O <sub>a</sub> )
<b>2c</b>	14.73	–17.12	–12.05	5.06	2.0494	2.2052
<b>2d</b>	14.84	–17.28	–12.02	5.25	2.0601	2.1870
<b>2e</b>	13.47	–14.10	–15.48	–1.38	2.0885 (Sn <sub>a</sub> –O <sub>a</sub> ) 2.1573 (Sn <sub>b</sub> –O <sub>b</sub> )	2.1497 (Sn <sub>a</sub> –O <sub>b</sub> ) 2.0829 (Sn <sub>b</sub> –O <sub>a</sub> )

<sup>a</sup> The calculated thermodynamic parameters (*H*, *S*, and *G*) are at 298.15 K and 1 atm. <sup>b</sup> Corrected by BSSE.



## Results and Discussion

**Selection of the Calculation Level of Theory.** To explore the calculation level of theory reliable for energy comparison, we first investigated the dialkoxide, Me<sub>2</sub>Sn(OMe)<sub>2</sub> (**1**), and its dimer **2** using various levels of theory (Scheme 1, Table 1). Accounting for the configuration of two terminal methoxy groups in **2**, eight dimeric formulations are possible (Figure 1). Three isomers (**2f–h**), however, are unstable and their stationary geometries could not be found under B3LYP/6-31G\*-LANL2DZ(Sn) level calculation. Among the other five energetically possible dimeric formulations (**2a–e**), **2a** is the most stable, in which both terminal methoxy groups are located in apical positions of the trigonal-bipyramidal tin atoms, consistent with the previous report of the crystal structure of **2a** (vide infra).<sup>4b</sup> Therefore, we initially concentrated on the calculation of **2a**.

As given in Table 1, The optimized Sn–O and Sn–C bond lengths at B3LYP and MP2 levels with LANL2DZ for Sn and 6-311+G\* for other atoms are in good agreement with the ones on the basis of X-ray analysis.<sup>4b</sup> At the HF level with the same basis set, the terminal Sn–O bonds are significantly shorter than the experimental ones. The shortening of the terminal Sn–O bond length is probably due to the nature of HF theory, i.e., the lack of electron correlation.

All of the enthalpy changes ( $\Delta H_{\text{corr}}$ ) and the free energy changes ( $\Delta G_{\text{corr}}$ ) corrected by a basis set superposition error (BSSE) are also listed in the table. For some calculations of the dimerization of **1**, the advantage of the free energy change was canceled out by BSSE. To minimize BSSE, the use of the larger basis set (e.g., aug-cc-p-VTZ-PP)<sup>15</sup> may be preferable, but consumes large computational resources. Notably, the  $\Delta H_{\text{corr}}$  and  $\Delta G_{\text{corr}}$  values at aug-cc-p-VDZ-PP,<sup>15</sup> which is a smaller basis set, are comparable to those at aug-cc-p-VTZ-PP. There-

fore, the BSSE-corrected energy calculated by using a basis set of medium size can be reasonably used to determine the direction of the dimerization/dissociation equilibrium.

Judging from experimental data of dibutyltin dialkoxide, the  $\Delta H_{\text{corr}}$  and  $\Delta G_{\text{corr}}$  values between **1** and **2a** at B3LYP and HF levels seem to be too high. That is, the calculated  $\Delta H_{\text{corr}}$  value at the B3LYP/6-311+G\*-LANL2DZ(Sn) level is less negative (–16.48 kcal mol<sup>-1</sup>) than the experimental  $\Delta H$  of more sterically crowded dibutyltin diisopropoxide (–24 kcal mol<sup>-1</sup>).<sup>6a</sup> Because the entropy term (*TΔS*) is not sensitively varied by the calculation level, the calculated  $\Delta G_{\text{corr}}$  value at B3LYP and HF levels turns positive, which is inconsistent with the experimental results. Interestingly, the chain length of the alkyl group bound to the tin atom was found to effect the energy change in an opposite manner between B3LYP and MP2. At B3LYP/6-311+G\*-LANL2DZ(Sn), the BSSE-corrected energy change ( $\Delta E_{\text{corr}}$ ) of the methyl derivative (**1** to **2a**) is lower than those of the ethyl and butyl derivatives (Table 2).<sup>16</sup> By contrast,  $\Delta E_{\text{corr}}$  at MP2/6-311+G\*-LANL2DZ(Sn) decreases as the alkyl chain becomes longer. At both calculation levels, the alkyl chains on the different tin atoms in the most stable dimer are contacted by each other.<sup>17</sup> In the butyl derivative, the dispersion force between alkyl chains should increase and the dimeric formulation should be more stabilized than in the methyl derivative. At the B3LYP level, however, the dispersion force would be poorly reproduced<sup>18</sup> and the repulsive force due to steric effect is predominant. From the above arguments, B3LYP is not suitable for making the monomer/dimer energy comparison in the tin alkoxide.<sup>19,20</sup>

(15) (a) Peterson, K. A. *J. Chem. Phys.* **2003**, *119*, 11099. (b) Metz, B.; Stoll, H.; Dolg, M. *J. Chem. Phys.* **2000**, *113*, 2563.

(16) For more detailed data including energies for the monomers and dimers, see the Supporting Information.

(17) See Supporting Information (Figure S-6).

(18) (a) Meijer, E. J.; Sprik, M. *J. Chem. Phys.* **1996**, *105*, 8684. (b) Cybulski, S. M.; Seversen, C. E. *J. Chem. Phys.* **2005**, *122*, 14117.

(13) (a) Simon, S.; Duran, M.; Dannenberg, J. J. *J. Chem. Phys.* **1996**, *105*, 11024. (b) Boys, S. F.; Bernardi, F. *Mol. Phys.* **1970**, *19*, 553.

(14) NBO, Version 3.1; Glendening, E. D.; Reed, A. E.; Carpenter, J. E.; Weinhold, F.

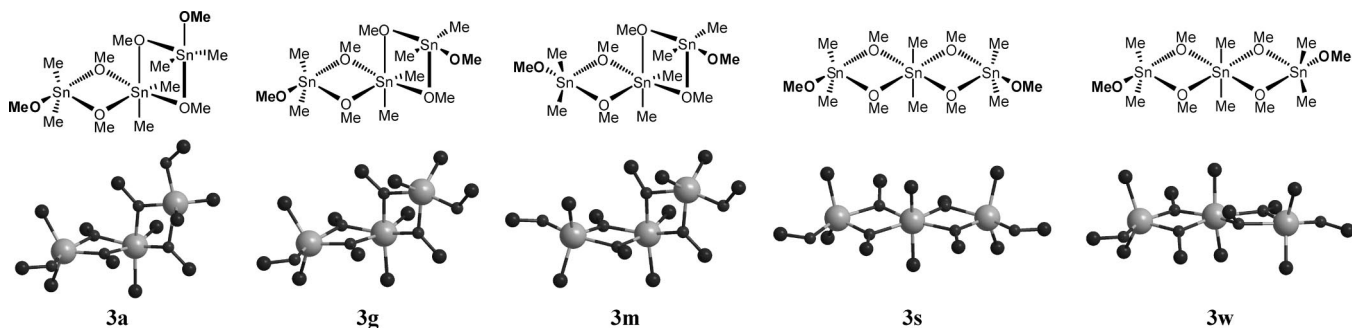


Figure 2. Optimized structures of **3a**, **3g**, **3m**, **3s**, and **3w** calculated by MP2/6-31G\*-LANL2DZ(Sn). Hydrogen atoms are omitted for clarity.

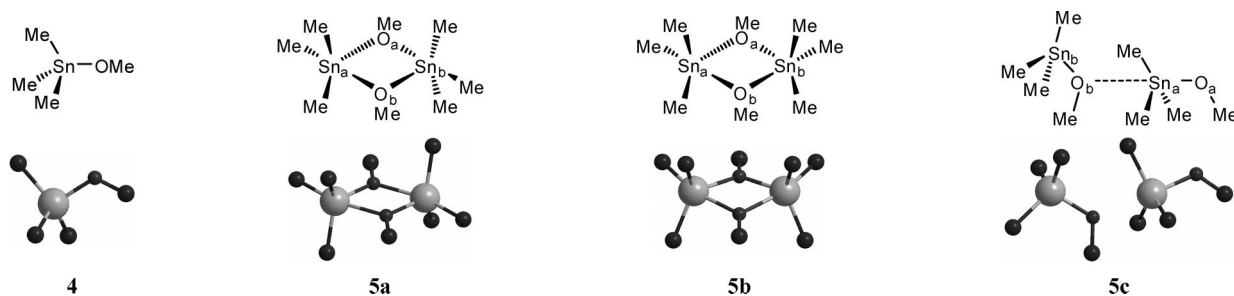


Figure 3. Optimized structures of **4** and **5a–c** calculated by MP2/6-311+G\*-LANL2DZ(Sn). Hydrogen atoms are omitted for clarity.

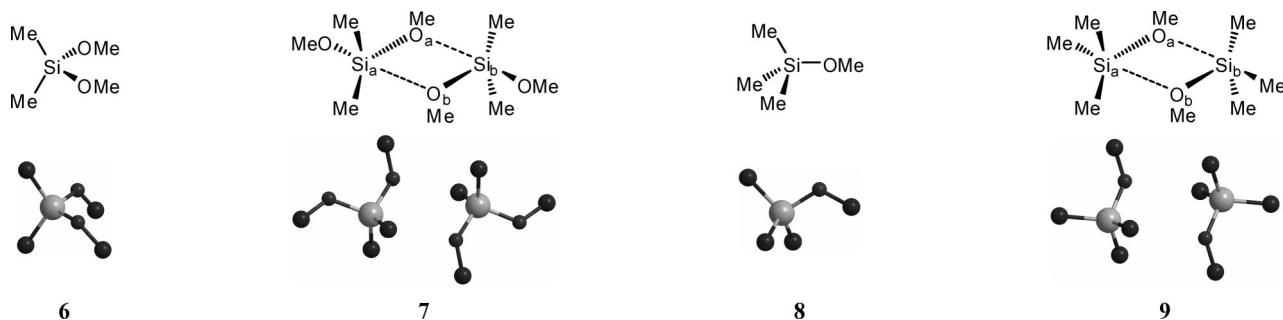


Figure 4. Optimized structures of **6–9** calculated by MP2/6-311+G\*-LANL2DZ(Sn). Hydrogen atoms are omitted for clarity.

Table 5. Calculation Results at MP2/6-31G\*-LANL2DZ(Sn) in Trimerization of **1** to **3<sup>a</sup>**

	BSSE/ kcal mol <sup>-1</sup>	<i>T</i> Δ <i>S</i> / kcal mol <sup>-1</sup>	Δ <i>H</i> <sub>corr</sub> <sup>b</sup> / kcal mol <sup>-1</sup>	Δ <i>G</i> <sub>corr</sub> <sup>b</sup> / kcal mol <sup>-1</sup>
<b>3a</b>	33.94	-33.25	-24.89	8.36
<b>3g</b>	33.95	-32.88	-24.31	8.57
<b>3m</b>	36.25	-33.17	-21.37	11.80
<b>3s</b>	31.16	-30.99	-20.28	10.71
<b>3w</b>	34.37	-31.89	-15.66	16.23

<sup>a</sup> The calculated thermodynamic parameters (*H*, *S*, and *G*) are at 298.15 K and 1 atm. <sup>b</sup> Corrected by BSSE.

To validate the energy calculated by MP2, we performed single-point energy calculations with several levels of theory, B3LYP, HF, MP2, MP3, and MP4(SDQ), using the MP2 optimized geometry (Table 3).<sup>16</sup> Δ*E*<sub>corr</sub> at the B3LYP level does not differ significantly from that at the HF level, but is lowered more than 4 kcal mol<sup>-1</sup> at the MP2 level. Such difference between B3LYP and MP2 probably arises from the difference in electron correlation. Electron correlation will shorten the

Table 6. Calculation Results at MP2/6-311+G\*-LANL2DZ(Sn) in Dimerization of **4** to **5<sup>a</sup>**

	BSSE/ kcal mol <sup>-1</sup>	<i>T</i> Δ <i>S</i> / kcal mol <sup>-1</sup>	Δ <i>H</i> <sub>corr</sub> <sup>b</sup> / kcal mol <sup>-1</sup>	Δ <i>G</i> <sub>corr</sub> <sup>b</sup> / kcal mol <sup>-1</sup>	Sn–O/Å
<b>4</b>					1.9637
<b>5a</b>	12.17	-17.36	-9.70	7.66	2.0376 (Sn <sub>a</sub> –O <sub>a</sub> ,
					Sn <sub>b</sub> –O <sub>b</sub> )
					2.3344 (Sn <sub>b</sub> –O <sub>a</sub> ,
Sn <sub>b</sub> –O <sub>a</sub> )					
<b>5b</b>	13.26	-17.04	-4.18	12.86	2.1403 (Sn <sub>a</sub> –O <sub>a</sub> ,
					Sn <sub>b</sub> –O <sub>a</sub> )
					2.1661 (Sn <sub>b</sub> –O <sub>b</sub> ,
Sn <sub>a</sub> –O <sub>b</sub> )					
<b>5c</b>	7.69	-15.53	-2.78	12.75	1.9994 (Sn <sub>a</sub> –O <sub>a</sub> ,
					1.9956 (Sn <sub>b</sub> –O <sub>b</sub> )
					2.6431 (Sn <sub>a</sub> –O <sub>b</sub> )

<sup>a</sup> The calculated thermodynamic parameters (*H*, *S*, and *G*) are at 298.15 K and 1 atm. <sup>b</sup> Corrected by BSSE.

Sn–O coordination bond and stabilize the dimeric formulation, because it diminishes the π-type antibonding interaction between

(19) (a) Recently, several papers reported that B3LYP fails to calculate accurate energy differences between hydrocarbon isomers: Grimme, S. *Angew. Chem., Int. Ed.* **2006**, *45*, 4460. (b) Wodrich, M. D.; Corminboeuf, C.; Schreiner, P. R.; Fokin, A. A.; Schleyer, P. v. R. *Org. Lett.* **2007**, *9*, 1851 and references cited therein.

(20) A theoretical study of homolytic substitution reactions of acyl radicals at tin has been reported: Matsubara, H. Schiesser, C. H. *Org. Biomol. Chem.* **2003**, *1*, 4335. They mentioned MP2 and higher levels of theories predict to favor frontside transition states while B3LYP does not.

**Table 7. Atomic Charge Evaluated by Natural Population Analysis with MP2 Density**

	Me <sub>2</sub> Sn(OMe) <sub>2</sub>		Me <sub>3</sub> SnOMe		Me <sub>2</sub> Si(OMe) <sub>2</sub>		Me <sub>3</sub> SiOMe	
	1 (monomer)	2a (dimer)	4 (monomer)	5a (dimer)	6 (monomer)	7 (dimer)	8 (monomer)	9 (dimer)
Sn or Si	2.41	2.50	2.25	2.35	2.22	2.25	2.04	2.05
O (bridged)	-0.96	-1.03	-0.95	-1.00	-0.93	-0.95	-0.92	-0.93
O (terminal)		-0.99				-0.94		

**Table 8. Calculation Results at MP2/6-311+G\*-LANL2DZ(Si) in Dimerization of the Silicon Analogues (6 and 8)<sup>a</sup>**

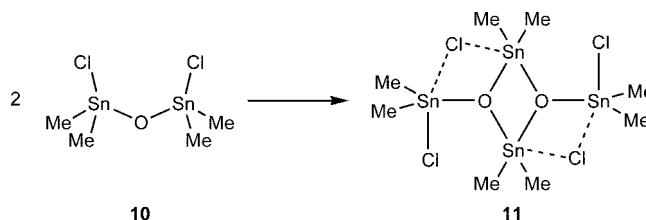
	BSSE/ kcal mol <sup>-1</sup>	TΔS/ kcal mol <sup>-1</sup>	ΔH <sub>corr</sub> <sup>b</sup> / kcal mol <sup>-1</sup>	ΔG <sub>corr</sub> <sup>b</sup> / kcal mol <sup>-1</sup>	Si-O/Å
6					1.7063, 1.7072
7	7.81	-10.06	-1.15	8.90	1.7051 (Si <sub>a</sub> -O <sub>a</sub> , Si <sub>b</sub> -O <sub>b</sub> ) 3.4006, 3.4158 (Si <sub>b</sub> -O <sub>a</sub> , Si <sub>b</sub> -O <sub>a</sub> )
8					1.7247
9	6.41	-10.53	-1.46	9.07	1.7328 (Si <sub>a</sub> -O <sub>a</sub> , Si <sub>b</sub> -O <sub>b</sub> ) 3.7380, 3.7426 (Si <sub>b</sub> -O <sub>a</sub> , Si <sub>b</sub> -O <sub>a</sub> )

<sup>a</sup> The calculated thermodynamic parameters (*H*, *S*, and *G*) are at 298.15 K and 1 atm. <sup>b</sup> Corrected by BSSE.

σ(Sn-C) and n(O) in HOMO of **2a**.<sup>21</sup> Generally, MP2 often overestimates the effect of electron correlation but it is improved by inclusion of the higher order of perturbation. In the calculation of **1** and **2a**, the Δ*E*<sub>corr</sub> values obtained by MP2, MP3, and MP4(SDQ) have been found to be nearly constant. Therefore, the MP2 energy is allowed to use energy comparison between the monomer and the dimer. As such, we used the MP2 theory with 6-311+G\*-LANL2DZ(Sn) basis sets except when specifically mentioned in the sections to follow.

**Dimethyltin Dimethoxide.** As mentioned above, there are five energetically possible dimeric formulations of dimethyltin dimethoxide. These calculation results are listed in Table 4.<sup>16</sup> The most stable **2a** experiences large exergonic Δ*G*<sub>corr</sub> variation (-7.37 kcal mol<sup>-1</sup>) upon dimerization of monomer **1** in spite of a relatively large entropy loss (*T*Δ*S* = -13.37 kcal mol<sup>-1</sup>). In **2a**, both terminal methoxy groups occupy apical positions of the trigonal-bipyramidal tin atoms, according to Muetterties' rule.<sup>22</sup> Two terminal methoxy groups are situated in an *anti* fashion, which is least sterically hindered among the five structures. The Sn-O bond is elongated from 1.9489 Å in monomer **1** to 2.0274 Å concomitant with formation of the longer coordination bond (2.2358 Å). The corresponding *syn* structure **2e** is less favored in terms of both enthalpy and entropy. Incorporation of methoxy group(s) at equatorial position(s) (**2b-d**) results in endergonic Δ*G*<sub>corr</sub> changes upon dimerization.

The conversion to trimers was also calculated at MP2 with LANL2DZ for Sn and 6-31G\* for other atoms (Scheme 2). As many as 26 structures are possible, all of which possess two four-membered rings with one six-coordinate central tin and two five-coordinate tin atoms.<sup>23</sup> The calculation results of five structures having only apical terminal methoxy groups are presented in Figure 2 and Table 5.<sup>16</sup> All of them, upon monomer-to-trimer conversion, encounter a positive Δ*G*<sub>corr</sub> value, which unambiguously proves that the dimer **2a** is much more favored than the trimer **3**. Consistent with the present theoretical outcome, the strong bias in favor of the dimeric

**Scheme 3****Table 9. Calculation Results at MP2/6-311+G\*-LANL2DZ(Sn) in Dimerization of the Distannoxanes (10 and 12)<sup>a</sup>**

dimer	BSSE/ kcal mol <sup>-1</sup>	TΔS/ kcal mol <sup>-1</sup>	ΔH <sub>corr</sub> <sup>b</sup> / kcal mol <sup>-1</sup>	ΔG <sub>corr</sub> <sup>b</sup> / kcal mol <sup>-1</sup>
11	27.76	-17.76	-25.10	-7.34
13a	22.29	-17.88	-49.13	-31.24
13b	26.25	-19.09	-37.16	-18.07

<sup>a</sup> The calculated thermodynamic parameters (*H*, *S*, and *G*) are at 298.15 K and 1 atm. <sup>b</sup> Corrected by BSSE.

species was previously put forth by NMR studies on dialkyltin dialkoxides with small alkoxy groups.<sup>6a,b</sup>

**Trimethyltin Monomethoxide.** Next, the monomer-to-dimer conversion of Me<sub>3</sub>SnOMe (**4**) was investigated (Figure 3 and Table 6).<sup>16</sup> Three dimeric formulations are possible: two with a four-membered ring (**5a** and **5b**) and the other with a simple donor-acceptor pair (**5c**). The conversions to all three dimers from monomer **4** are endergonic (positive Δ*G*<sub>corr</sub>). Upon formation of a four-membered ring in **5a** and **5b** from monomer **4**, the enthalpy gain, though substantially large, yields the entropic disadvantage (*T*Δ*S* = ca. -17 kcal mol<sup>-1</sup>) while formation of the simple tin-oxygen coordination bond in **5c** cannot earn enough enthalpy gain despite competition against the relatively small entropic disadvantage (*T*Δ*S* = -15.53 kcal mol<sup>-1</sup>). The predominance of the monomer over aggregated species for various trialkyltin alkoxides has been reported previously on the basis of NMR spectroscopy.<sup>6a,b</sup>

**Atomic Charges.** The atomic charges evaluated by natural population analysis (NPA) of the monomers (**1**, **4**) and the dimers (**2a**, **5a**) are listed in Table 7. The charge density at tin in the dimethoxide monomer **1** is higher than that in the monomethoxide **4** whereas little difference appears at oxygen. It follows that the increase in the Lewis acidity of the tin atom plays a primary role for formation of the tin-oxygen coordination bond. Notably, the charge density at tin is slightly increased upon dimer formation. A similar tendency was reported for conversion of four-coordinate silicon species to five-coordinate fluorosilicates.<sup>24</sup>

For comparison, putative dimerization of Me<sub>2</sub>Si(OMe)<sub>2</sub> (**6**) and Me<sub>3</sub>SiOMe (**8**) was simulated (Figure 4 and Table 8).<sup>16</sup> No stable dimer formation was suggested in any case. The charge density at silicon in monomer **6** is lower than that in the tin analogue **1** (Table 7), due to the smaller electronegativity. On the other hand, the charge density at oxygen in **6** is hardly changed from **1**. Therefore, the degree of Lewis acidity of the tin atom is a dominant factor for association.

(21) See Supporting Information (Figure S-7).

(22) Muetterties, E. L.; Mahler, W.; Schmutzler, R. *Inorg. Chem.* **1963**, *2*, 613.

(23) See Supporting Information (Tables S-10, S-11, and S-12). It should be noted that no six-membered ring is plausible.

(24) Deiters, J. A.; Holmes, R. R. *J. Am. Chem. Soc.* **1990**, *112*, 7197.

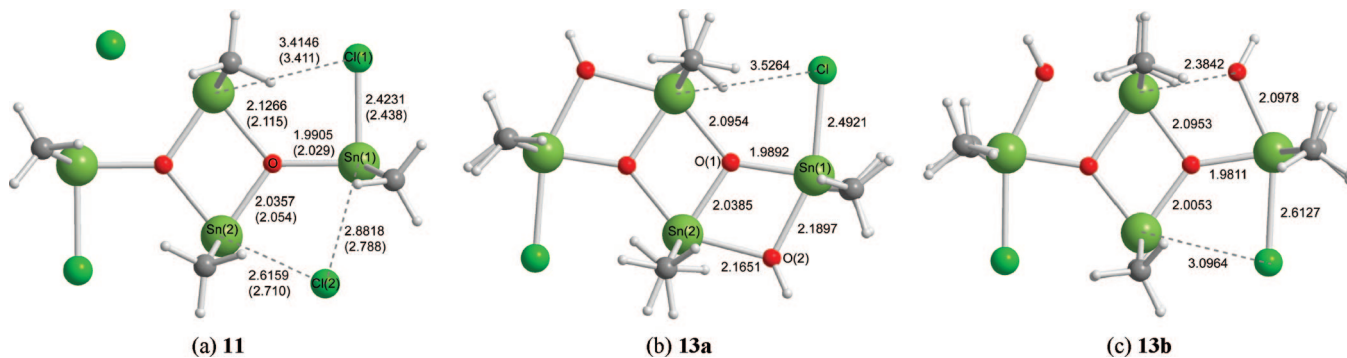
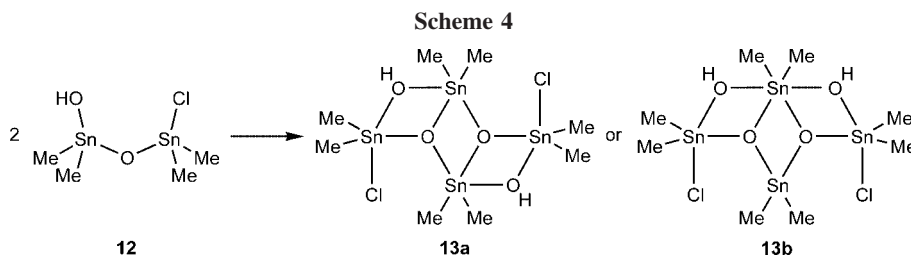


**Figure 5.** Optimized structures of **11**, **13a**, and **13b** calculated by MP2/6-311+G\*-LANL2DZ(Sn). Some atomic distances are also indicated in Å. The values in parentheses are experimental.<sup>7d</sup>



**Distannoxane.** Formation of distannoxane dimer **11** from monomer **10** gives rise to a large negative  $\Delta G_{\text{corr}}$  value ( $-7.34 \text{ kcal mol}^{-1}$ ) consistent with the well-known stable dimeric association (Scheme 3 and Table 9).<sup>16</sup> Similar to dimeric dimethyltin dimethoxide (**2a**), the large enthalpy gain ( $\Delta H_{\text{corr}} = -25.10 \text{ kcal mol}^{-1}$ ), which is enough to compensate for the entropy loss ( $T\Delta S = -17.76 \text{ kcal mol}^{-1}$ ), causes the stabilization of the dimeric distannoxane. The bond lengths of optimized structure **11** are in good agreement with those obtained by X-ray analysis<sup>7d</sup> (Figure 5a). Notably, the Sn(2)–Cl(2) bond is almost ionized in accordance with the X-ray study. The calculated charges at tin are 2.28 (**10**), 2.29 (Sn(1) in **11**), and 2.41 (Sn(2) in **11**), respectively. The tin atoms in **10** are less positive than that in the dimethyltin dimethoxide monomer **1** (2.41, Table 7). On the other hand, as expected, the oxygen atom between the tin atoms in **10** has a higher negative charge density ( $-1.43$ ) than that in **1** ( $-0.96$ , Table 7). This indicates that the oxygen at **10** has a stronger Lewis basicity, and is reflected on the shortening of the secondary Sn–O bond (2.1266 Å for **11** vs 2.2358 Å for **2a**). Much greater dimer stabilization was revealed for hydroxydistannoxane **13a** (Scheme 4 and Table 9): the  $\Delta G_{\text{corr}}$  value of the monomer-to-dimer conversion is  $-31.24 \text{ kcal mol}^{-1}$ . The optimized structure is similar to the reported X-ray structure of the tetraisopropyldistannoxane derivative.<sup>7f</sup> Significantly, the hydroxy groups occupy the bridging positions to give a perfect ladder structure, which may be responsible for a slight increase in entropic disadvantage ( $T\Delta S = -17.88 \text{ kcal mol}^{-1}$ ) as compared with **11** (Figure 5b). However, the entropic change is outweighed by a large enthalpy gain ( $\Delta H = -49.13 \text{ kcal mol}^{-1}$ ) arising from formation of the additional Sn–O bonds. The *syn* isomer (**13b**) was also calculated and found less

stable than **13a**, though its  $\Delta G_{\text{corr}}$  value is still largely negative ( $-18.07 \text{ kcal mol}^{-1}$ ) (Figure 5c).

## Conclusions

In conclusion, we have shown that ab initio calculations at the MP2/6-311+G\*-LANL2DZ(Sn) level provide reliable information about structure and bonding of organotin molecules. The association behavior of organotin alkoxides is counterbalanced by conflicting enthalpy and entropy contributions. The increase in Lewis acidity of tin induced by attachment of alkoxy group(s) is of prime importance for the association. On the other hand, formation of the stable dimeric distannoxanes has been proved by great negative  $\Delta G$  values. The oxygen atom between the tin atoms in distannoxanes has stronger Lewis basicity than that in organotin alkoxides. The multiplier effect of both Lewis acidity of tin and Lewis basicity of oxygen is reflected in the shortening of the secondary Sn–O bond. On the basis of the results obtained here, we are now further developing the present approach to elucidate reaction mechanisms involving organotin alkoxides and distannoxanes.

**Supporting Information Available:** Complete tables including energies of the molecules in hartrees, figures for optimized structures of dialkyltin dimethoxides (Me, Et, Bu), a figure for HOMO of **2a**, optimized coordinates and energies from Gaussian Archive entries in output files, and a complete reference 11 containing a full author list. This material is available free of charge via the Internet at <http://pubs.acs.org>.

OM701179J